

The Effect of Luminous Lens Blending in Gravitational Microlensing Experiments

Seunghun Lee, Cheongho Han

Dept. of Astronomy & Space Science,
Chungbuk National University, Cheongju, Korea 361-763
cheongho@astro.chungbuk.ac.kr, leess@astro.chungbuk.ac.kr

Received _____; accepted _____

ABSTRACT

The most important uncertainty in the results of gravitational microlensing experiments comes from the difficulties of photometry caused by blending of source stars. Recently Nemiroff (1997) pointed out that the results of microlensing experiments can also be affected by the blending of light from the lens itself if a significant fraction of lenses are composed of stars. In this paper, we estimate the effects of lens blending on the optical depth determination and the derived matter distribution toward the Galactic bulge by using realistic models of the lens matter distribution and a well-constrained stellar luminosity function. We find that the effect of lens blending is largest for lenses located in the Galactic disk. However, lens blending does not seriously affect both the determination of the optical depth and the Galactic matter distribution. The decrease in optical depth is $\sim 10\%$ even under the extreme assumption that lenses are totally composed of stars and disk matter distribution follows a maximal disk model, in which the lens blending effect is most severe.

Subject headings: The Galaxy — gravitational lensing — dark matter — Stars: low-mass

submitted to *The Astrophysical Journal*: July ??, 1997
Preprint: CNU-A&SS-03/97

1. Introduction

Large surveys trying to detect gravitational microlensing events by monitoring stars located in the Large Magellanic Cloud (LMC) and the Galactic bulge are being carried out by the MACHO (Alcock et al. 1997), EROS (Renault et al. 1996), OGLE (Udalski et al. 1994), and DUO (Alard, Mao, & Guibert 1995) groups. They have already detected ~ 20 candidate events toward the LMC and $\gtrsim 150$ events toward the Galactic bulge (Gould, private communication).

The results of these lensing experiments are typically presented in terms of optical depth. By definition, the optical depth represents the average fraction of the sources that is being gravitationally amplified more than a factor of 1.34 at any given time. For a given model of lens matter distribution, $\rho(D_{\text{ol}})$, the optical depth is theoretically determined by

$$\tau = \frac{4\pi G}{c^2} \int_0^{D_{\text{os}}} dD_{\text{ol}} \rho(D_{\text{ol}}) \frac{D_{\text{ol}} D_{\text{ls}}}{D_{\text{os}}}, \quad (1.1)$$

where D_{ol} , D_{ls} , and D_{os} are the separations between the observer, lens, and source. Observationally, on the other hand, the optical depth is determined by

$$\tau = \frac{\pi}{2N_* T} \sum_{j=1}^{N_{\text{event}}} \frac{t_{\text{E},j}}{\epsilon_j}, \quad (1.2)$$

where N_* and N_{event} are, respectively, the total numbers of monitored stars and detected events, T is the total observation time, and $\epsilon(t_{\text{E}})$ is the detection efficiency. Here the Einstein time scale represents the required time for a source star to cross the Einstein ring radius r_{E} ,

$$t_{\text{E}} = \frac{r_{\text{E}}}{v}; \quad r_{\text{E}} = \left(\frac{4GM}{c^2} \frac{D_{\text{ol}} D_{\text{ls}}}{D_{\text{os}}} \right)^{1/2}, \quad (1.3)$$

and its value is obtained by fitting theoretical light curve to the measured one. The theoretical light curve is related to the lensing parameters by

$$A_{\text{abs}} = \frac{u^2 + 2}{u(u^2 + 4)^{1/2}}; \quad u = \left[\beta^2 + \left(\frac{t - t_0}{t_{\text{E}}} \right)^2 \right]^{1/2}, \quad (1.4)$$

where u is the lens-source separation in units of r_{E} , β is the impact parameter of the lens-source encounter, and t_0 is the time of maximum amplification. From the comparison of the theoretical and observed optical depths, one can obtain precious information about the MACHO-type matter fraction within the Galaxy. In addition, analysis of the optical depth distribution for various lines of sight provides an important tool for the study of Galactic structure (Sackett & Gould 1993; Han & Gould 1995).

However, precise determination of the optical depth is hampered by blending problem. Due to the blended light from background stars that are not participating in the event, the apparent amplification of an event is lower than its absolute value. As a result, the

apparent Einstein time scale is shorter than its true value. Since the optical depth is directly proportional to the time scale, the optical depth determined without proper correction of blending effect is systematically underestimated (Di Stefano & Esin 1995; Wozniak & Paczyński 1997).

Recently, Nemiroff (1997) pointed out that not only background source stars but also bright stellar lenses cause blending, ‘lens blending’. The light from bright lenses causes the measured optical depth to be underestimated by the same way as blending by unresolved background stars does. In addition, he showed that due to the lens blending the detection of events caused by lenses closer to the observer is comparatively more difficult than the detection of events produced by lenses near the source. This latter effect of lens blending causes the matter distribution derived from the optical depth distribution to deviate from its true value.

In this paper, we estimate the effects of lens blending on the optical depth determination and the derived matter distribution toward the Galactic bulge by using realistic models of the lens matter distribution and a well-constrained stellar luminosity function. We find that the effect of lens blending is largest for lenses located in the Galactic disk. However, lens blending does not seriously affect both the determination of the optical depth and the Galactic matter distribution. The decrease in optical depth is $\sim 10\%$ even under the extreme assumption that lenses are totally composed of stars and disk matter distribution follows a maximal disk model, in which the lens blending effect is most severe.

2. Blending by Bright Lenses

If a source star is gravitationally lensed by another star, the absolute amplification, A_{abs} , of the event is diluted by the light from the lens, and the event appears to be amplified by

$$A_{\text{app}} = \frac{A_{\text{abs}}l_S + l_L}{l_S + l_L}, \quad (2.1)$$

where l_L and l_S are the apparent fluxes of the lens and the source and A_{abs} is the absolute amplification. Due to this dilution of amplification, the measured event time scale appears to be shorter than its true value by a factor

$$\eta = \left[2 \left(1 - A_{\text{min}}^{-2} \right)^{-1/2} - 2 \right]^{1/2}; \quad A_{\text{min}} = 1.34 \left(1 + \frac{l_L}{l_S} \right) - \left(\frac{l_L}{l_S} \right), \quad (2.2)$$

where A_{min} is the minimum required amplification for detection (Nemiroff 1997). Since the optical depth is directly proportional to the time scale, τ is decreased by the same factor by the lens blending.

In addition, lens blending makes the distribution of lenses causing events along the line of sight toward a direction differ from its true one. In general, the lens matter distribution does not coincide with the matter distribution. This difference between the lens and matter

distributions arises because the cross-section of the lens-source encounter, i.e., Einstein ring diameter $2r_E$, depends on the geometry of the lens system by equation (1.3). For a uniform distribution of matter, the lensing probability peaks at the very center between the observer and the source star, and it decreases as the lens approaches either the source or the lens. In addition to this intrinsic dependence on the lens system geometry, the optical depth distribution additionally depends on the lens location due to the effect of lens blending. This additional dependency on lens geometry arises because stellar lenses that are nearby, and thus apparently brighter, cause more blending than those near the sources do (Nemiroff 1997). Therefore, the factor by which the optical depth is decreased depends not only on the relative absolute lens/source flux ratio, L_L/L_S , but also on the lens geometry, i.e.,

$$\eta\left(\frac{L_L}{L_S}, \frac{D_{\text{os}}}{D_{\text{ol}}}\right) = \left[2\left(1 - A'_{\text{min}}{}^{-2}\right)^{-1/2} - 2\right]^{1/2}; \quad A'_{\text{min}} = 1.34 \left[1 + \frac{L_L}{L_S} \left(\frac{D_{\text{os}}}{D_{\text{ol}}}\right)^2\right] - \frac{L_L}{L_S} \left(\frac{D_{\text{os}}}{D_{\text{ol}}}\right)^2. \quad (2.3)$$

3. Models of Matter Distribution and Luminosity Function

Since the effect of lens blending depends on both the lens geometry and the lens/source flux ratio, it is required to model the Galactic matter distribution and the luminosity function of stars for the estimation of the lens blending effect on actual lensing experiments. In addition, the fraction of stellar lenses among all types (dark+luminous) of lenses should be known. However, all these quantities required to estimate the lens blending effect are poorly known. Therefore, we test various models of matter distribution, lens brightness, and stellar lens fraction.

A fraction of events toward the LMC might be caused by stars in the Galactic disk and in the LMC itself (Sahu 1994). However, this fraction of events is $\lesssim 10\%$ of the total events expected from all-MACHO halo (Wu 1994). On the other hand, a significant fraction of events toward the Galactic bulge lenses is thought to be caused by stars (Kamionkowski 1995; Han, Chang, & Lee 1997). Therefore, we estimate the effect of the lens blending only on the experiments which are being carried out toward the Galactic bulge.

We test two bulge matter distribution models. First, we adopt the axisymmetric Kent bulge model (Kent 1992) of the form,

$$\rho(s) = \begin{cases} 1.04 \times 10^6 (s/0.482)^{-1.85} M_{\odot} \text{ pc}^{-3}, & (\text{for } s < 938 \text{ pc}), \\ 3.53 K_0 (s/667) M_{\odot} \text{ pc}^{-3}, & (\text{for } s \geq 938 \text{ pc}), \end{cases} \quad (3.1)$$

where $s^4 = R^4 + (z/0.61)^4$, $R = (x^2 + y^2)^{1/2}$, and the axes x and z are directed toward the observer and toward the Galactic pole from the Galactic center, respectively. The second COBE bulge model (Dwek et al. 1995) has a triaxial shape, or bar-shaped, with an analytic form of

$$\rho(r_s) = \rho_{0,\text{COBE}} \exp(0.5r_s^2) M_{\odot} \text{ pc}^{-3}, \quad (3.2)$$

where $r_s = \{[(x'/x_0)^2 + (y'/y_0)^2]^2 + (z'/z_0)^4\}^{1/4}$ and $(x_0, y_0, z_0) = (1.58, 0.62, 0.43)$ kpc. The coordinates (x', y', z') represent axes of the bar from the longest to the shortest, and the longest axis is misaligned with the x axis by an angle of 20° . We set the normalization to be $\rho_{\text{COBE}} \sim 2.0 \times 10^9 M_\odot \text{ pc}^{-3}$ so that the total mass of the bulge matches with the Zhao et al.'s (1995) estimate of $2.0 \times 10^{10} M_\odot$.

For the Galactic disk matter distribution, we adopt a double exponential disk of the form

$$\rho(R, z) = 0.06 \exp \left\{ - \left[\frac{R - 8000}{h_R} + \frac{z}{h_z} \right] \right\} M_\odot \text{ pc}^{-3}, \quad (3.3)$$

where the radial and vertical scale heights are $h_R = 3.5$ kpc and $h_z = 325$ pc (Bahcall 1986). Since the events caused by stars in the disk are more likely to be affected by the lens blending effect compared to those caused by relatively remote bulge stars, we also test the maximal disk model. In the maximal disk model, matter is distributed in the same way as in the Bahcall disk model, but the distribution has 3 times higher normalization. The adopted matter distribution models of the Galactic structures are summarized in Table 1.

By using these models, we test 3 combinations of Galactic matter distribution. These combinations are Kent bulge + Bahcall disk (model I), COBE bulge + Bahcall disk (model II), and Kent bulge + maximal disk (model III) as listed in Table 2. The matter distributions along the line of sight toward Baade's Window located at $(\ell, b) = (1^\circ, -3^\circ.9)$ for these three Galactic mass distribution models are shown in Figure 1. One finds that model II has lower disk/bulge matter ratio compared to model I distribution, while model III has higher ratio.

The I -band luminosity function of stars is constructed by combining ground (J. Frogel, private communication) and space-based observations (R. M. Light, private communication). In addition, we extend the very faint part of the luminosity function by adopting that of stars in the solar neighborhood (Gould, Bahcall, & Flynn 1996). For the construction of the luminosity function, we assume that the populations of stars in the disk and bulge are similar each other. The finally constructed luminosity function is presented in Fig 1 of Han (1997).

4. Estimate of Lens Blending Effect

Based on the models of Galactic mass distribution and the luminosity function, the optical depth distribution taking lens blending into consideration is computed by

$$\frac{d\tau(D_{\text{ol}})}{dD_{\text{ol}}} = \frac{4\pi G}{c^2} \rho(D_{\text{ol}}) \int_{D_{\text{ol}}}^{d_{\text{max}}} dD_{\text{os}} \eta \left(\frac{L_L}{L_S}, \frac{D_{\text{os}}}{D_{\text{ol}}} \right) n(D_{\text{os}}) \frac{D_{\text{ol}} D_{\text{ls}}}{D_{\text{os}}} \times \left[\int_{D_{\text{ol}}}^{d_{\text{max}}} dD_{\text{os}} n(D_{\text{os}}) \right]^{-1}, \quad (4.1)$$

where $n(D_{\text{os}}) \propto \rho(D_{\text{os}})$ is the number density of source stars and $d_{\text{max}} = 12$ kpc is the upper limit of the source star distribution. Above equation differs from equation (1.1) because source stars are distributed in a wide spatial range, and thus their locations can no longer

be approximated as a constant. The term in the bracket ([]) is included to normalize the lensing probability for a single source star. In addition, by setting the lens mass density to be the sum of disk and bulge densities, i.e., $\rho = \rho_{\text{disk}} + \rho_{\text{bulge}}$, we include both disk-bulge and self-lensing (disk-disk and bulge-bulge) event contribution in the optical depth computation.

Recently Han et al. (1997) determined the fraction of Galactic bulge events caused by stars to be $f_* \lesssim 50\%$. Therefore, in our computation we assume 50% of events are due to stellar lenses, and the other 50% of events are caused by dark component of lenses. However, the luminous lens fraction is still very uncertain. Therefore, we also test two other cases of lens fractions in which stars comprise 70% and 100% of total lenses. In the computation, we choose the brightnesses of lenses from the model luminosity function by a Monte Carlo method. On the other hand, source star brightnesses are selected from the part of the luminosity function brighter than the I -band absolute magnitude of $M_I = 4$, which is the detection limit of ground based observation. This is because while stars at any brightness can work as lenses, to be monitored source stars should be bright enough to be resolved overcoming the threshold detection limit imposed by the blending of stars.

The optical depth distributions for individual mass distribution models are computed by equations (2.3) and (4.1), and they are shown in the upper panels of Figure 2. In each panel, we compute the optical depth distributions with the stellar lens fractions of $f_* = 50\%$ (dotted line), 70% (short-dashed line), and 100% (long-dashed line), and they are compared to the distribution obtained without any lens blending effect, i.e., $f_* = 0\%$, (solid line). To better show the slight differences in the optical depth distributions for different values of stellar lens fraction, the sections of distributions in the range $2 \text{ kpc} \leq D_{\text{ol}} \leq 4 \text{ kpc}$ are magnified and presented in the middle panels. In addition, the total optical depths for individual mass distribution models with (and without) the lens blending effect are computed by

$$\tau_{\text{with(w/o)}} = \int_0^{d_{\text{max}}} \frac{\tau(D_{\text{ol}})}{dD_{\text{ol}}} dD_{\text{ol}}, \quad (4.2)$$

and they are listed in Table 3.

One finds that the blending effect on optical depth distribution mainly occurs for disk lenses as pointed out by Nemiroff (1997). This can be easily seen in the optical depth distribution ratio, $d\tau_{\text{with}}(D_{\text{ol}})/d\tau_{\text{w/o}}(D_{\text{ol}})$, shown in the lower panels of Figure 2. As the disk/bulge mass ratio increases, lensing events are more likely to be affected by lens blending, resulting in smaller values of optical depth. For example, the ratio between the total optical depths with and without considering the blending effect for the model III mass distribution is smaller than that of model I. However, for a fixed stellar lens fraction the decreases in optical depth for different mass distribution models are similar one another regardless of the assumed models. That is, lens blending effect is fairly mass-distribution independent. On the other hand, lens blending effect has relatively strong dependency on the assumed stellar lens fractions. Under model I mass distribution, for example, the optical depth ratio is $\tau_{\text{with}}/\tau_{\text{w/o}} = 94.3\%$ if half of lenses are composed of stars, i.e., $f_* = 50\%$, while $\tau_{\text{with}}/\tau_{\text{w/o}} = 88.8\%$ for pure stellar lenses, i.e., $f_* = 100\%$.

However, the result of lensing experiments is not seriously affected by the lens blending. The decrease in optical depth is just $\sim 5\%$ for the most probable stellar lens fraction of $f_* = 50\%$. Even for the extreme case where the lenses are totally composed of stars and the disk matter follows the maximal distribution, in which the lens blending has maximum effect, the decrease in τ is $\sim 13.5\%$. The reason for this small effect of lens blending is that although a significant fraction of lenses can be composed of stars, most of them are very faint. On the other hand, the source stars being monitored by current lensing experiments are relatively very bright compared to typical stellar lenses. Therefore, the approximation of dark lenses is still good enough for the current experiments' purpose of determining dark matter fraction and studying Galactic structures.

We would like to thank S. Gaudi & A. Berlind for making precious comments and suggestions.

REFERENCES

- Alard, C., Mao, S., & Guibert, J. 1995, *A&A*, 300, L17
- Alcock, C., et al. 1997, *ApJ*, 479, 119
- Bahcall, J. N. 1986, *ARA&A*, 24, 577
- Di Stefano, R., & Esin, A. 1995, *ApJ*, 448, 1
- Dwek, E., et al. 1995, *ApJ*, 445, 716
- Gould, A., Bahcall, J., & Flynn, C. 1996, *ApJ*, 465, 759
- Han, C. 1997, *ApJ*, 484, 555
- Han, C., Chang, K., & Lee, S. 1997, *ApJ*, submitted (astro-ph/9705137)
- Han, C., & Gould, A. 1995, *ApJ*, 449, 521
- Kamionkowski, M. 1995, *ApJ*, 442, L9
- Kent, S. M. 1992, *ApJ*, 387, 181
- Nemiroff, R. J. 1997, *ApJ*, submitted (astro-ph/9704114)
- Renault, C. et al. 1996, *A&A*, submitted (astro-ph/9612102)
- Sackett, P., & Gould, A. 1993, *ApJ*, 419, 648
- Sahu, K. C. 1994, *Nature*, 370, 275
- Udalski, A., et al. 1994, *AcA*, 44, 165
- Wozniak, P., & Paczyński, B. 1997, *ApJ*, submitted (astro-ph/9702194)
- Wu, X-P. 1994, *ApJ*, 435, 66
- Zhao, H., Spergel, D. N., & Rich, R. M. 1995, *ApJ*, 440, L13

TABLE 1
THE MATTER DENSITY DISTRIBUTION MODELS

| model | distribution |
|--------------|---|
| bulge | |
| Kent | $\rho(s) = 1.04 \times 10^6 (s/0.482)^{-1.85} M_{\odot} \text{ pc}^{-3}$ (for $s < 938$ pc) $\rho(s) = 3.53 K_0 (s/667) M_{\odot} \text{ pc}^{-3}$ (for $s \geq 938$ pc) |
| COBE | $\rho(r_s) = 2.0 \times 10^9 \exp(0.5r_s^2) M_{\odot} \text{ pc}^{-3}$ |
| disk | |
| Bahcall | $\rho(R, z) = 0.06 \exp\{ -[(R - 8000)/3500 + z/325] \} M_{\odot} \text{ pc}^{-3}$ |
| Maximal | $\rho(R, z) = 0.18 \exp\{ -[(R - 8000)/3500 + z/325] \} M_{\odot} \text{ pc}^{-3}$ |

NOTE.— The model Galactic bulge and disk matter distributions. In the Kent bulge model, $s^4 = R^4 + (z/0.61)^4$, $R = (x^2 + y^2)^{1/2}$, and x and z axes direct toward the observer and toward the Galactic pole. In the COBE bulge model, $r_s = \{[(x'/x_0)^2 + (y'/y_0)^2]^2 + (z'/z_0)^4\}^{1/4}$, where $(x_0, y_0, z_0) = (1.58, 0.62, 0.43)$ kpc, and x' and z' represent the longest and shortest axes of the triaxial bulge. For both bulge models, the normalizations are set so that the total mass of the bulge is $M_{\text{bulge}} \sim 2 \times 10^{10} M_{\odot}$. In the maximal disk model, matter is distributed the same way as in the Bahcall disk model, but has 3 times higher normalization.

TABLE 2
THE GALACTIC MASS DISTRIBUTION MODEL

| model | component | |
|-------|-----------|---------|
| | bulge | disk |
| I | Kent | Bahcall |
| II | COBE | Bahcall |
| III | Kent | Maximal |

NOTE.— The Galactic mass distribution models. They are obtained from the combination of the Galactic bulge and disk models listed in Table 1.

TABLE 3
THE EFFECT OF LENS BLENDING ON OPTICAL DEPTH DETERMINATION

| f_* (%) | mass model | τ_{with} (10^{-6}) | $\tau_{\text{w/o}}$ (10^{-6}) | $\tau_{\text{with}}/\tau_{\text{w/o}}$ (%) |
|--------------|---------------|---------------------------------------|--------------------------------------|---|
| 50% | I | 1.018 | 1.079 | 94.3 |
| | II | 1.334 | 1.411 | 94.5 |
| | III | 1.684 | 1.808 | 93.1 |
| 70% | I | 0.994 | 1.079 | 92.1 |
| | II | 1.304 | 1.411 | 92.4 |
| | III | 1.636 | 1.808 | 90.5 |
| 100% | I | 0.958 | 1.079 | 88.8 |
| | II | 1.259 | 1.411 | 89.2 |
| | III | 1.564 | 1.808 | 86.5 |

NOTE.— The effect of lens blending on the determination of the optical depth. Here f_* represents the stellar lens fraction among all (luminous+dark) types of lenses. Therefore, the stellar lens fraction of 100% represents that lenses are totally composed of pure stars.

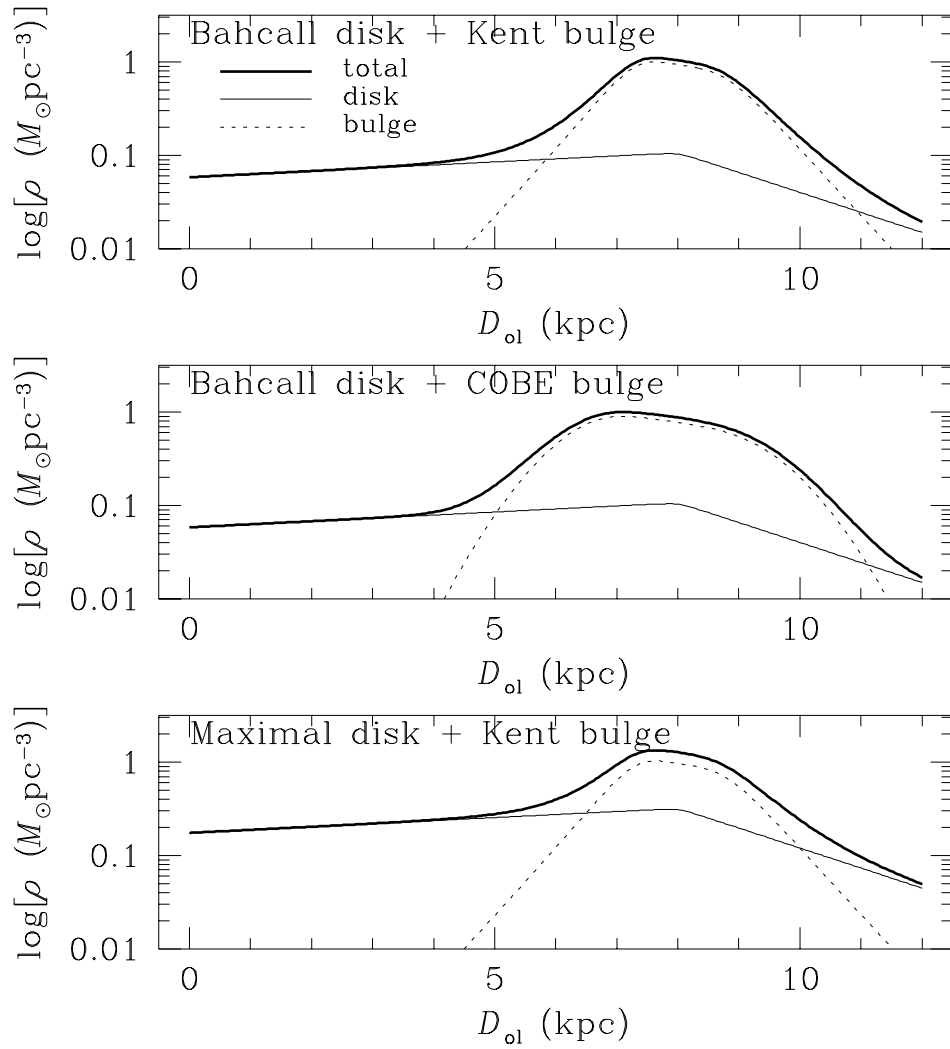


Figure 1: The mass distributions along the line of sight toward Baade’s Window for various Galactic mass distribution models listed in Table 2. The distributions of the bulge and disk matter are represented, respectively, by thin dotted and solid lines, and the thick solid represents the sum of both distributions.

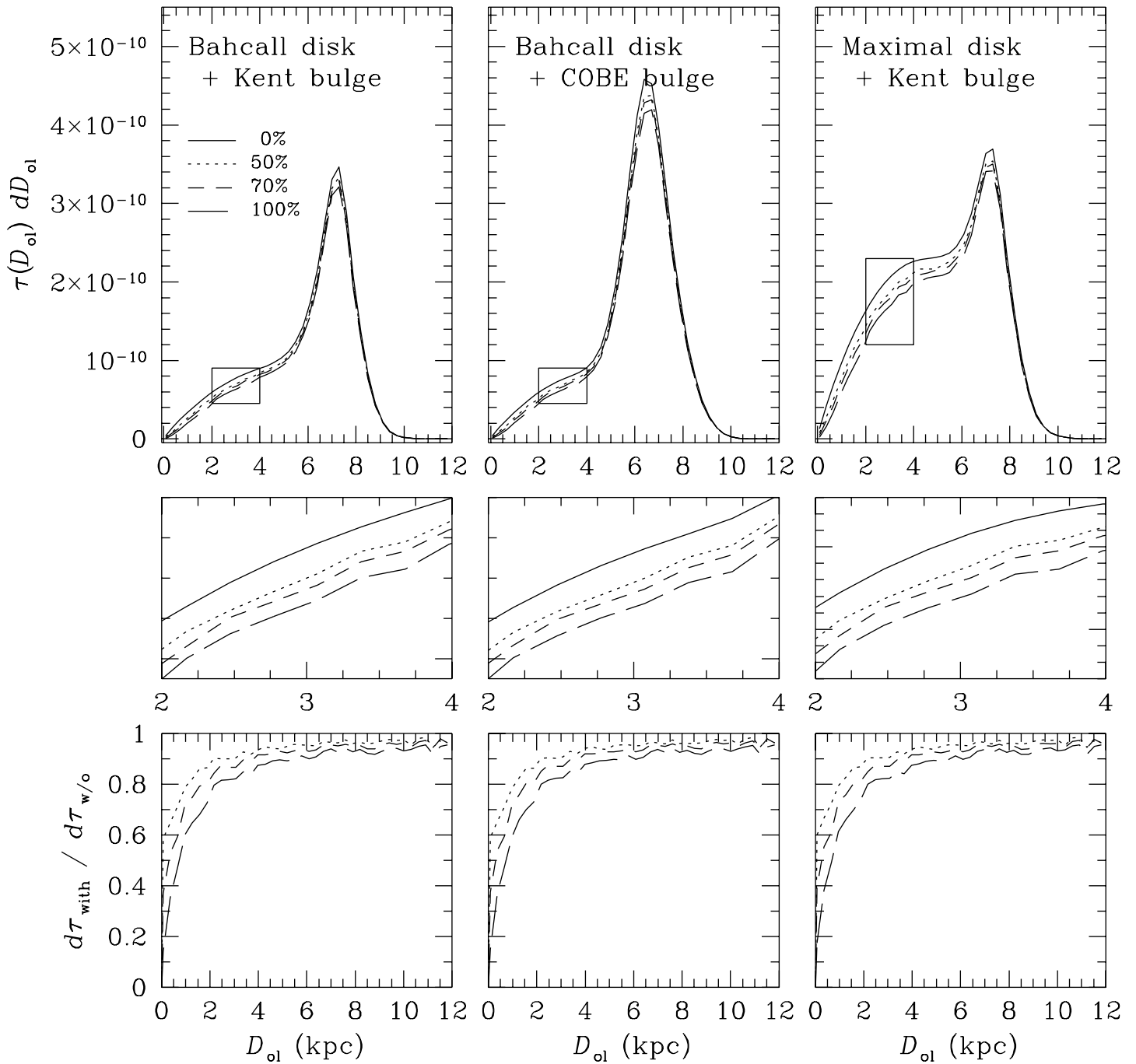


Figure 2: The optical depth distributions for various models of Galactic mass distribution and stellar lens fractions. To better show the slight differences in the optical depth distribution, the sections of small boxes in the individual upper panels are magnified and shown in corresponding middle panels. Also shown in the lower panels are the ratios between the optical depth distribution with and without the blending effect.